# Accuracy of Dispersion Interactions In Semi-empirical and Molecular Mechanics Models: The Benzene Dimer Case.

**ARTICLE** *in* THE JOURNAL OF PHYSICAL CHEMISTRY A · SEPTEMBER 2014

Impact Factor: 2.69 · DOI: 10.1021/jp506860t · Source: PubMed



**3 AUTHORS**, INCLUDING:

Manuel Melle-Franco
University of Minho
**43** PUBLICATIONS **904** CITATIONS

SEE PROFILE

THE JOURNAL OF PHYSICAL CHEMISTRY A

Article

pubs.acs.org/JPCA

# Accuracy of Dispersion Interactions in Semiempirical and Molecular Mechanics Models: The Benzene Dimer Case

Karol Strutyński,[†] José A. N. F. Gomes,[†] and Manuel Melle-Franco*[,‡]

[†]REQUIMTE, Departamento de Química, Faculdade de Ciências, Universidade do Porto, Rua do Campo Alegre S/N, 4169-007 Porto, Portugal

[‡]Departamento de Informática, Centro de Ciências e Tecnologias da Computação, Universidade do Minho, 4710-057 Braga, Portugal

Supporting Information

**ABSTRACT:** The benzene dimer is arguably the simplest molecular analogue of graphitic materials. We present the systematic study of minima and transition states of the benzene dimer with semiempirical and molecular mechanics (MM) methods. Full minimizations on all conformations were performed and the results, geometries, and binding energies were compared with CCSD(T) and DFT-D results. MM yields the best results with three force fields MM3, OPLS, and AMOEBA, which reproduced nine out of the ten stationary points of the benzene dimer. We obtained new parameters for MM3 and OPLS that successfully reproduce all structures of the benzene dimer and showed improved accuracy over DFT-D in most dimer geometries. Semiempirical models were, unexpectedly, less accurate than MM methods. The most accurate semiempirical method for the benzene dimer is PM6-DH2. DFT-D was the only Hamiltonian that reproduced the variations of energy with geometry from CCSD(T) calculations accurately and is the method of choice for energies of periodic and molecular calculations of graphitic systems. In contrast, MM represents an accurate alternative to calculate geometries.

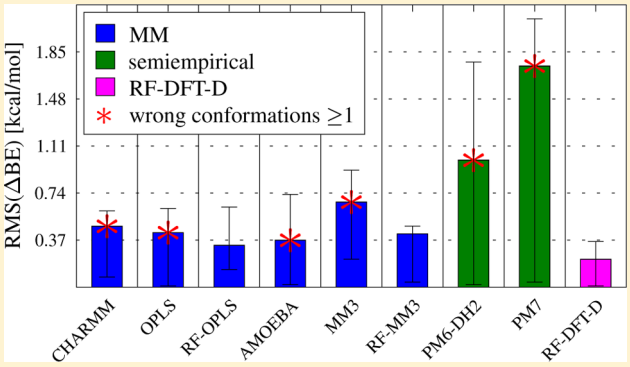


## INTRODUCTION

Carbon nanomaterials like fullerenes,[1] carbon nanotubes,[2−4] and graphene[5,6] have explosively developed into a very active field of research in which computer models have played a fundamental role. van der Waals (vdW) interactions are the driving force for the packing of graphitic materials; from graphite to carbon nanotubes[7] passing trough multishell fullerenes,[8] multiwall carbon nanotubes[9] and carbon peapods.[10−12] van der Waals forces are also fundamental for modeling the interaction of graphitic materials with their environment, for instance with nanoliquids,[13,14] biological membranes,[15] and proteins[16] and in noncovalent functionalization.[17,18]

Dispersion interactions are intrinsically hard to model with ab initio quantum methods. The models that describe them with consistently good accuracy (e.g., coupled cluster methods[19−21]) are feasible only for small molecules. Density functional theory (DFT) models are more popular as they are orders of magnitude more efficient. In a previous work we analyzed how accurately different DFT Hamiltonians reproduce dispersion interactions in the benzene dimer.[22] In the present work we will extend that study to semiempirical and molecular mechanics models.

Benzene dimer (BD) is arguably the simplest molecular analogue of graphite. Experimental data on the benzene dimer are scarce: the interaction energy is about −2.4 kcal/mol,[23] and although the exact geometry of the BD is not experimentally known, the minimum is most likely a T-shaped structure.[24]

In contrast, the benzene dimer has been the object of many theoretical investigations that also yielded a very shallow binding.[25−28] Most recent and accurate theoretical studies yield two almost isoenergetic minima ($PD_a$ and $TT_b$) and, at least, eight transition states (Figure 1).[27,29]

Graphite and the benzene dimer share the same dispersion interactions. In fact, models with accurate dispersion on BD are also accurate on graphite.[22] The weak binding together with the availability of highly accurate data make benzene dimer a stringent test for dispersion for polyaromatic hydrocarbons and, ultimately, for graphite.

## METHODS

The accuracy of models with very different computational costs, namely density functional theory, semiempirical methods, and molecular mechanics methods against reference data at the CCSD(T) level will be presented. The same methodology and metrics used in our previous work on DFT models was used.[22]

The CCSD(T) method is widely considered the gold standard of quantum chemistry models and was used as

**Received:** July 9, 2014
**Revised:** September 9, 2014
**Published:** September 10, 2014

   dx.doi.org/10.1021/jp506860t | J. Phys. Chem. A 2014, 118, 9561−9567

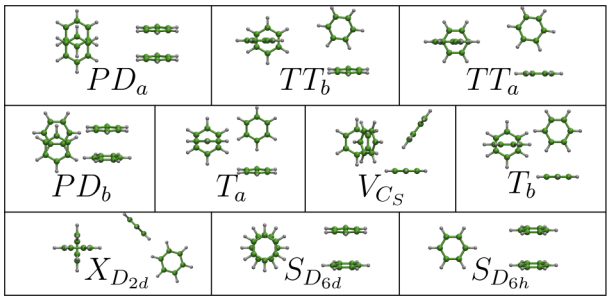


**Figure 1.** Benzene dimer conformations: parallel displaced (PD), sandwich type (S), T-shaped (T), tilted T-shaped (TT), V-shaped (V), and X-shaped (X) configurations. The subscript of the configuration indicates the symmetry of the molecule or the position of one molecule with respect to the other (a, over atom; b, over bond).

reference; stationary points and their binding energies were extrapolated to the complete basis set calculated at the CCSD(T)/aug-cc-pVDZ level,[27] and the potential energy surface (PES) was calculated at the CCSD(T)/aug-cc-pVQZ* level of theory.[25] DFT calculations were run with a home version of NWchem 6.1.1[30] that is available on request. Semiempirical calculations were performed with MOPAC 2012.[31,32] Molecular mechanics calculations were run with the Tinker software suite.[33−35]

## RESULTS

To quantify the capacity to reproduce geometries and binding energies of BD minima and transition states for all Hamiltonians, we performed full geometry optimizations starting from CCSD(T) geometries. The differences in binding energy between the reference CCSD(T) data and the investigated methods are shown in Table 1. Table 2 quantifies the ability to reproduce the CCSD(T) geometries. Metrics based on root-mean-square differences in molecular structures and energies for all the conformations with stable stationary points are included as an indicator of overall performance for each method.

**DFT-D Method.** DFT-D methods are based on DFT Hamiltonians augmented with a classical $1/R^6$ dispersion term.[36,37] DFT-D has already been used to study the benzene dimer.[26,38] Recently, we presented a new set of DFT-D parameters for BD derived to be applicable in periodic quantum chemistry calculations.[22] Those parameters were obtained using a relaxed fiting (RF) procedure where the geometries are relaxed within the fitting scheme and consequently follow the optimization of the parameters. DFT-D parameters obtained from relaxed fitting (RF-DFT-D) yield improved accuracy and robust parameters. In fact, RF-DFT-D using the BLYP functional was one of the most accurate DFT models for benzene dimer as found by the authors.[22] For simplicity we will only discuss here a DFT-D parametrization with a double-ζ basis set,[a] as it is computationally more efficient. Note that the RF-DFT-D parameters with larger basis sets are substantially more accurate.[22]

**Semiempirical Methods.** Semiempirical (SE) Hamiltonians are based on the Hartree−Fock formalism with a number of approximations. Most notably, some computationally expensive integrals are fitted to experimental data. Similarly to DFT, SE methods were recently augmented with classical corrections. The SE-D methods presented in this study are PM6-DH2[39] and PM6-DH+[40] (which are equivalent for the benzene dimer) and the recent PM7.[41] In addition to SE-D methods, we also tried AM1,[42] RM1,[43] MNDO,[44] and PM6,[31] which, due to poor performance, will be reported in the Supporting Information.

PM7 and PM6-DH2 are generally overbinding and fail to to reproduce some BD conformations. PM7 favors sandwich type conformations over PD conformations (Table 1), and consequently, the $PD_a$ minimum is not reproduced. PM6-DH2 yields improved energetics and fails only with two conformations, $TT_a$ and $V_{C_s}$ (the latter being a problematic conformation for most models). For the sandwich conformations, interaction energies are too binding with errors up to 100% and 180% for PM6-DH2 and PM7, respectively.

**Molecular Mechanics.** Molecular mechanics models are typically based on point particles centered on atomic nuclei interacting via mathematical functions fitted to reproduce empirical and/or quantum derived properties. We have studied all force fields available in the TINKER suite with explicit aromatic carbon parameters, namely, MM2,[45] MM3,[46] CHARMM22,[47−49] OPLS,[50] and MMFF[51] force fields. Additionally, two polarizable models, the model for benzene by Dang[52,53] and the AMOEBA09 force field,[54−56] were included.

The intermolecular interactions in benzene dimer in MM are described by the sum of the Coulumbic and van der Waals

**Table 1. Binding Energy Errors**[a]

| | | | | | | | RF | | | BE |
|---|---|---|---|---|---|---|---|---|---|---|
| conf | CHARMM | OPLS | AMOEBA | MM3 | PM6-DH2 | PM7 | OPLS | MM3 | DFT-D | CCSD(T) |
| $PD_a$ | −0.53 | −0.62 | 0.06 | −0.22 | 0.88 | **2.09** | −0.22 | −0.43 | −0.33 | −2.73 |
| $TT_b$ | −0.54 | −0.51 | −0.21 | −0.86 | 0.02 | 0.53 | −0.17 | −0.46 | −0.01 | −2.82 |
| $TT_a$ | −0.54 | −0.51 | −0.19 | −0.85 | **0.03** | 0.54 | −0.16 | −0.44 | 0.02 | −2.80 |
| $PD_b$ | **−0.43** | **−0.46** | 0.04 | −0.22 | 0.88 | **2.11** | −0.22 | −0.42 | −0.30 | −2.72 |
| $T_a$ | −0.60 | −0.55 | −0.55 | −0.92 | −0.09 | 0.62 | −0.14 | −0.41 | −0.08 | −2.70 |
| $V_{C_s}$ | −0.45 | −0.48 | **0.02** | **−0.24** | **0.86** | **2.09** | −0.15 | −0.43 | −0.03 | −2.74 |
| $T_b$ | −0.19 | −0.16 | 0.19 | −0.45 | 0.44 | 0.93 | 0.20 | −0.04 | 0.36 | −2.40 |
| $X_{D_{2d}}$ | −0.39 | −0.38 | −0.73 | −0.78 | −0.32 | −0.04 | −0.30 | −0.38 | 0.29 | −1.79 |
| $S_{D_{6d}}$ | 0.09 | −0.01 | 0.37 | 0.66 | 1.77 | 3.12 | 0.63 | 0.48 | 0.14 | −1.71 |
| $S_{D_{6h}}$ | 0.08 | −0.02 | 0.33 | 0.64 | 1.75 | 3.11 | 0.62 | 0.48 | 0.15 | −1.71 |
| RMS | 0.43 | 0.42 | 0.37 | 0.67 | 1.00 | 1.74 | 0.33 | 0.42 | 0.22 | |

[a]Positive values indicate energies that are more binding than the reference ($BE_{CCSD(T)}$). The root mean square (RMS) gives a measure of the overall accuracy. Values in bold show conformations that switch during geometry optimization. All values are in kcal/mol.


dx.doi.org/10.1021/jp506860t | J. Phys. Chem. A 2014, 118, 9561−9567

**Table 2. Root Mean Square Deviation of the Optimized Geometries (RMSD, Å) and the Root Mean Square (RMS) for Each Method Presented as a Measure of the Overall Performance[a]**

| | | | | | | | RF | | |
|---|---|---|---|---|---|---|---|---|---|
| conf | CHARMM | OPLS | AMOEBA | MM3 | PM6-DH2 | PM7 | OPLS | MM3 | DFT-D |
| $PD_a$ | 0.40 | 0.41 | 0.05 | 0.01 | 0.16 | $\mathbf{S_{D_{6h}}}$ | 0.07 | 0.05 | 0.12 |
| $TT_b$ | 0.12 | 0.09 | 0.19 | 0.15 | 0.23 | 0.15 | 0.05 | 0.07 | 0.11 |
| $TT_a$ | 0.11 | 0.09 | 0.22 | 0.16 | $\mathbf{T_b}$ | 0.13 | 0.05 | 0.07 | 0.11 |
| $PD_b$ | $\mathbf{V_{C_s}}$ | $\mathbf{V_{C_s}}$ | 0.06 | 0.01 | 0.19 | $\mathbf{S_{D_{6d}}}$ | 0.07 | 0.05 | 0.12 |
| $T_a$ | 0.07 | 0.05 | 0.07 | 0.09 | 0.07 | 0.07 | 0.03 | 0.05 | 0.04 |
| $V_{C_s}$ | 0.29 | 0.15 | $\mathbf{PD_b}$ | $\mathbf{PD_b}$ | $\mathbf{PD_b}$ | $\mathbf{S_{D_{6d}}}$ | 0.05 | 0.01 | 0.08 |
| $T_b$ | 0.03 | 0.02 | 0.01 | 0.04 | 0.11 | 0.12 | 0.05 | 0.08 | 0.07 |
| $X_{D_{2d}}$ | 0.06 | 0.05 | 0.12 | 0.19 | 0.02 | 0.02 | 0.02 | 0.04 | 0.02 |
| $S_{D_{6d}}$ | 0.06 | 0.06 | 0.15 | 0.13 | 0.19 | 0.06 | 0.06 | 0.06 | 0.07 |
| $S_{D_{6h}}$ | 0.06 | 0.06 | 0.14 | 0.12 | 0.19 | 0.06 | 0.06 | 0.06 | 0.07 |
| RMS | **0.29** | **0.29** | **0.28** | **0.24** | **0.31** | **0.37** | 0.05 | 0.06 | 0.09 |

[a]For switched conformations, the new conformation is indicated in bold.

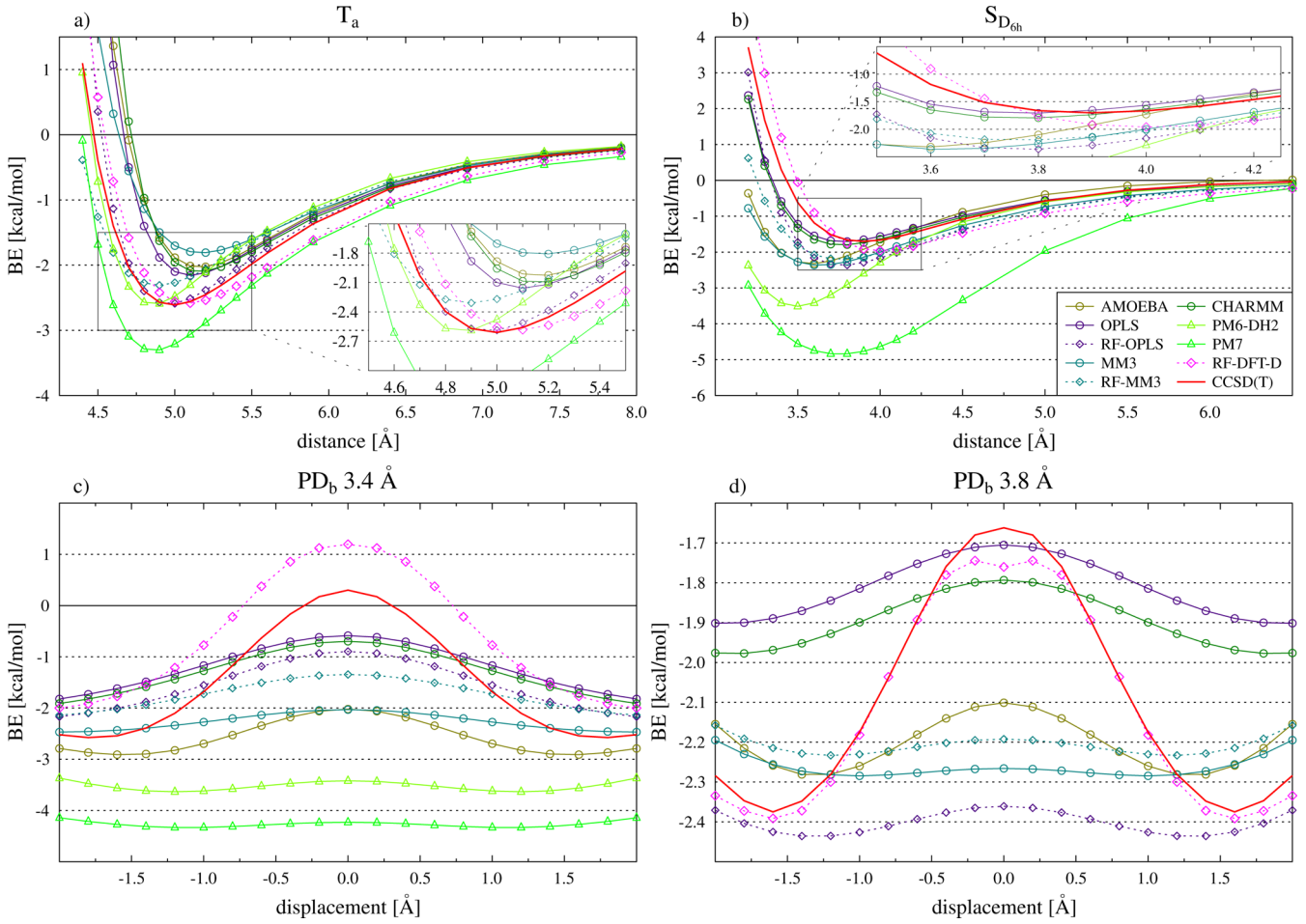


**Figure 2.** Binding energies (BE [kcal/mol]) of the potential energy surface of benzene dimer. For the $T_a$ and $S_{D_{6h}}$ conformations the center of mass distance is plotted on the *X*-axis, for the $PD_b$ conformations it indicates the displacement of the benzene molecules. The SE-D curves for $PD_b$ 3.8 Å are not shown, as they are strongly overbinding, and are presented in the Supporting Information.

terms. The Coulumbic interactions are calculated from point charges that are fitted to reproduce the electrostatic potential around the molecule derived from quantum calculations. The vdW term includes an attractive $1/R^6$ term and a repulsive term resulting from the electron density overlap that gives atoms, in these classical models, their volume. In fact, for BD, the energetics and geometries in MM models and in DFT-D arise from the balance between electrostatic forces and dispersion attractive interaction. In addition, intermolecular polarization adds a third term for polarizable models. The MM3, AMOEBA, CHARMM, and OPLS force fields are accurate and will be discussed here (the full table with results for all MM models


dx.doi.org/10.1021/jp506860t | J. Phys. Chem. A 2014, 118, 9561−9567

can be found in the Supporting Information). Interestingly, MM3, AMOEBA, CHARMM, and OPLS all fail in one conformation, either $PD_b$ or $V_{C_s}$ that is unstable over the other. The quality of geometries, which do not switch, are quite similar for all force fields and PM6-DH2. AMOEBA and MM3 produce the best energies and geometries, outclassing DFT-D geometries in some cases. We refined the vdW parameters for benzene with the relax fitting procedure in the OPLS and MM3 force fields. For the intermolecular interactions the MM3 and OPLS share the same point charges but differ in the vdW potentials; OPLS has a Lennard-Jones type potential with an $1/R^{12}$ repulsive term, whereas MM3 has Buckingham type potential with an exponential term. Both force fields have parameters for many small organic molecules but differ in scope. MM3 intermolecular interactions for aromatic carbon were fitted to several crystals and graphite.[57] Benzene parameters in OPLS were fitted to reproduce experimental observables from benzene liquid trough Monte Carlo simulations.[50] Also MM3 includes the semiempirical Parisser−Pople−Par Hamiltonian that is able to reproduce fullerenes and polyaromatic hydrocarbons bond alternation.

Binding energies for RF-OPLS and RF-MM3 show increased accuracy yet inferior to RF-DFT-D. Interestingly, the accuracy of the dimer geometries is highly improved (Table 2) and similar to or better than that for RF-DFT-D in most cases.

Lennard-Jones type potentials are unable to account for the energy difference between AA and AB graphite.[58] In the following section we will study this issue with potential energy surface (PES) calculations.

**Potential Energy Surfaces.** The energy of T-shaped and sandwich BD conformations at increasing distances and the sliding of benzene in the parallel displaced (PD) conformation were studied and are shown in Figure 2. All methods reproduce the overall shape of the PES for $T_a$ (Figure 2a) and $S_{D_{6h}}$ (Figure 2b) conformations. This is not surprising, as these curves correspond to the dissociation of the dimer and all vdW interactions sharing a $1/R^6$ term produce qualitatively similar results. The largest discrepancy is for SE-D methods, which show too large binding energies for the $S_{D_{6h}}$ conformations.

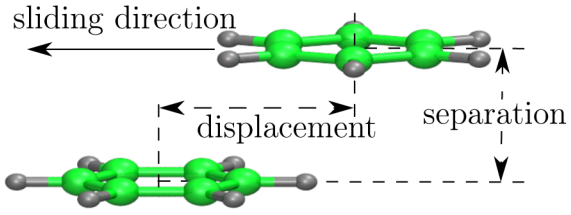


**Figure 3.** Sliding motion of the $PD_b$ conformation.

Figure 3 shows the geometric parameters of the sliding motion that transforms the $PD_b$ into the $S_{D_{6d}}$ conformation. The benzene molecules are separated by 3.5 Å in the $PD_b$ conformation (with the displacement of 1.70 Å), and 3.9 Å for the $S_{D_{6d}}$ conformation. For the sliding motion (Figure 2c,d), the best performance is for RF-DFT-D followed by MM models with Lennard-Jones potentials, namely OPLS, RF-OPLS, and CHARMM, followed by AMOEBA and RF-MM3. The MM3 energy profile is too smooth whereas PM6-DH2 and PM7 profiles are wrong as they favor sandwich conformations over PD ones[b]. All methods except the RF-DFT-D systematically underestimate the energy difference between both conformations at all separations. Also for most MM models in this study, sandwich and parallel displaced structures yielded similar energies whereas in CCSD(T) they differ by 1 kcal/mol. This is also the reason why binding energies are typically more accurate for one of those conformations than the other (compare Figure 2 with Table 1).

A registry-dependent intermolecular potential with an anisotropic term aimed to reproduce $\pi$ orbitals repulsive interactions reproduces accurately the sliding in graphite with molecular mechanics.[58] The fact that RF-OPLS and RF-MM3, though improving geometries and energetics, still fail to reproduce the PES is due to limitations of the repulsive terms of the potentials. Furthermore, this limitation accounts for the frictionless motion observed in encapsulated fullerenes with MM models.[10]

As a final test, we studied the PES of the $C_{60}$−benzene complex using RF-DFT-D, SE-D, and MM (a full description of these results is available in the Supporting Information).

In the PES, the benzene is situated over a [5,6] bond and then the fullerene is rotated perpendicular to the [5,6] bond (Figure 4). The results are presented in Figure 5. The RF-DFT-D minimum corresponds to the conformations in which the benzene is above a [6,6] bond. RF-MM3 and PM6-DH2 produce average interaction energies similar to that produced by the RF-DFT-D method but yield an energy profile that is too smooth. The energies more similar to RF-DFT-D are obtained for RF-MM3, vouching for the transferability of RF-MM3 parameters. RF-OPLS, CHARMM, and OPLS are too repulsive and are not binding.

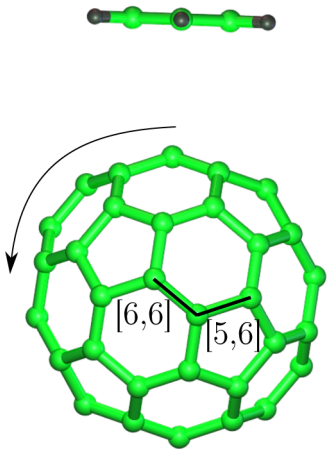


**Figure 4.** Potential energy surface geometries for the $C_{60}$−benzene complex (direction of fullerene rotation).

## CONCLUSIONS

The RF-DFT-D and relax fitted force fields (RF-MM3 and RF-OPLS) were able to reproduce the geometries of all stationary points of the benzene dimer with good accuracy. The MM3, OPLS, and AMOEBA failed only in one stationary point. Despite the improvement, the RF reparametrized force fields were unable to reproduce the energetics of the sliding motion in parallel displaced conformations. This is likely due to intrinsic limitations of vdW interaction used in each model. In most cases, the SE-D methods were less accurate than MM3 or OPLS, which are the method of choice after DFT-D. The most


dx.doi.org/10.1021/jp506860t | J. Phys. Chem. A 2014, 118, 9561−9567

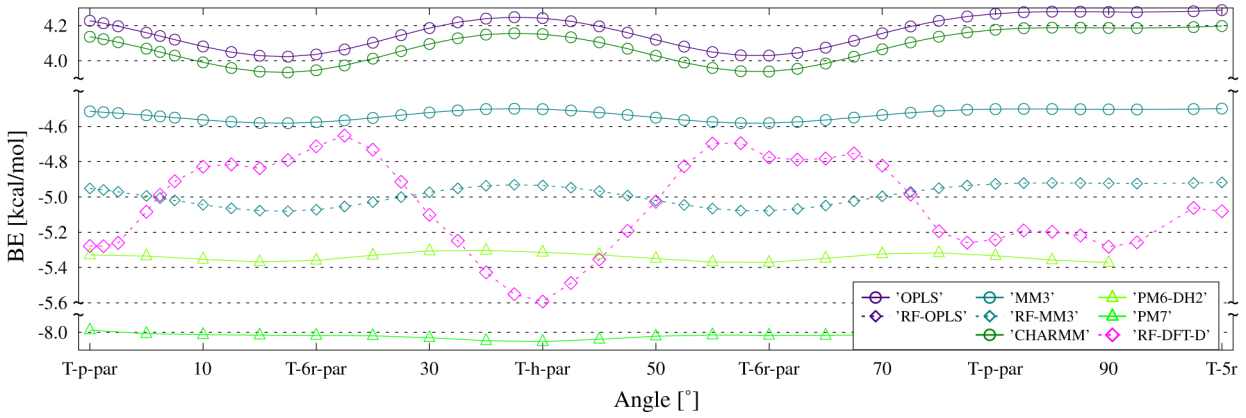


**Figure 5.** Binding energy (BE [kcal/mol]) of the $C_{60}$–benzene scan. The angle corresponds to rotations of the fullerene along the $C_2$ axis so that the benzene faces both types of fullerene bonds and rings. OPLS and CHARMM produced interaction energies around +4 kcal/mol, for the RF-OPLS force field interaction energies are around +2.6 kcal/mol. The AMOEBA force field calculations failed to converge and are not shown.

accurate SE method was PM6-DH2. In the PES of the $C_{60}$–benzene complex, RF-MM3 and PM6-DH2 showed binding energies similar to those of RF-DFT-D but still failed to reproduce its variations. RF-DFT-D is the method of choice of this study as it gives good geometries and reasonable energetics in all tests. MM3/OPLS/CHARM/AMOEBA/PM6-DH2 perform similarly, yet AMOEBA is not suitable for periodic systems (the polarization algorithm is not suitable for infinite systems). Unexpectedly, the SE methods perform worse than MM. For this reason, we advise the use of PM6-DH2 only for systems lacking parameters for MM.

Summing up, MM models, and specifically relax fitted models, are able to reproduce CCSD(T) calculated BD geometries with high accuracy. In contrast, DFT-D was the only method found to yield accurate binding energetics. MM or SE methods are not advised for accurate, relative or absolute, interaction energies of graphitic materials. RF-MM3 is the advised method for MM calculations. For computational efficiency, we recommend single point calculations at the DFT-D level on MM obtained geometries.

## ■ ASSOCIATED CONTENT

### Supporting Information

Tables and figures of binding energies obtained from all methods investigated. Description of the relaxed fitting method and parameters, and the full description of the $C_{60}$-benzene system. This material is available free of charge via the Internet at http://pubs.acs.org

## ■ AUTHOR INFORMATION

### Corresponding Author

*M. Melle-Franco. Phone: +351-253604459. E-mail: manuelmelle@gmail.com.

### Notes

The authors declare no competing financial interest.

## ■ ACKNOWLEDGMENTS

Financial support from *Fundação para a Ciência e Tecnologia* doctoral grant no. SFRH/BD/61894/2009, REQUIMTE PEst-C/EQB/LA0006/2011, the program Ciência 2008 and contracts PEst-OE/EEI/UI0752/2014 and CONC-REEQ/443/2005 are gracefully acknowledged.

## ■ ADDITIONAL NOTES

[a]The data for the benzene dimer presented here corresponds to the RF-6/6-31G in the original paper.
[b]SE-D results for $PD_b$ 3.8 Å are not shown, as they were highly overbinding.

## ■ REFERENCES

(1) Kroto, H. W.; Heath, J. R.; O'Brien, S. C.; Curl, R. F.; Smalley, R. E. $C_{60}$: Buckminsterfullerene. *Nature* **1985**, *318*, 162–163.
(2) Iijima, S.; Ichihashi, T. Single-Shell Carbon Nanotubes of 1-nm Diameter. *Nature* **1993**, *363*, 603–605.
(3) Bethune, D. S.; Klang, C. H.; de Vries, M. S.; Gorman, G.; Savoy, R.; Vazquez, J.; Beyers, R. Cobalt-Catalysed Growth of Carbon Nanotubes with Single-Atomic-Layer Walls. *Nature* **1993**, *363*, 605–607.
(4) Monthioux, M.; Kuznetsov, V. L. Who Should Be Given the Credit for the Discovery of Carbon Nanotubes? *Carbon* **2006**, *44*, 1621–1623.
(5) Novoselov, K. S.; Geim, A. K.; Morozov, S. V.; Jiang, D.; Zhang, Y.; Dubonos, S. V.; Grigorieva, I. V.; Firsov, A. A. Electric Field Effect in Atomically Thin Carbon Films. *Science* **2004**, *306*, 666–669 PMID: 15499015.
(6) Geim, A. K.; Novoselov, K. S. The Rise of Graphene. *Nat. Mater.* **2007**, *6*, 183–191.
(7) Melle-Franco, M.; Prato, M.; Zerbetto, F. Permanent Chiral Twisting of Nonchiral Carbon Nanotubes. *J. Phys. Chem. A* **2002**, *106*, 4795–4797.
(8) Cioffi, C.; Palkar, A.; Melin, F.; Kumbhar, A.; Echegoyen, L.; Melle-Franco, M.; Zerbetto, F.; Rahman, G. M.; Ehli, C.; Sgobba, V.; et al. A Carbon Nano-Onion–Ferrocene Donor–Acceptor System: Synthesis, Characterization and Properties. *Chem. - Eur. J.* **2009**, *15*, 4419–4427.
(9) Bellarosa, L.; Bakalis, E.; Melle-Franco, M.; Zerbetto, F. Interactions in Concentric Carbon Nanotubes: the Radius vs the Chirality Angle Contributions. *Nano Lett.* **2006**, *6*, 1950–1954.
(10) Melle-Franco, M.; Kuzmany, H.; Zerbetto, F. Mechanical Interactions in All-Carbon Peapods. *J. Phys. Chem. B* **2003**, *107*, 6986–6990.
(11) Chamberlain, T. W.; Pfeiffer, R.; Howells, J.; Peterlik, H.; Kuzmany, H.; Kräutler, B.; Da Ros, T.; Melle-Franco, M.; Zerbetto, F.; Milić, D.; et al. Engineering Molecular Chains in Carbon Nanotubes. *Nanoscale* **2012**, *4*, 7540.
(12) Chamberlain, T. W.; Pfeiffer, R.; Peterlik, H.; Kuzmany, H.; Zerbetto, F.; Melle-Franco, M.; Staddon, L.; Champness, N. R.; Briggs, G. A. D.; Khlobystov, A. N. Polyarene-Functionalized Fullerenes in Carbon Nanotubes: Towards Controlled Geometry of Molecular Chains. *Small* **2008**, *4*, 2262–2270.

(13) Catheline, A.; Ortolani, L.; Morandi, V.; Melle-Franco, M.; Drummond, C.; Zakri, C.; Pénicaud, A. Solutions of Fully Exfoliated Individual Graphene Flakes in Low Boiling Point Solvents. *Soft Matter* **2012**, *8*, 7882−7887.
(14) Melle-Franco, M.; Zerbetto, F. Ejection Dynamics of a Simple Liquid from Individual Carbon Nanotube Nozzles. *Nano Lett.* **2006**, *6*, 969−972.
(15) Höfinger, S.; Melle-Franco, M.; Gallo, T.; Cantelli, A.; Calvaresi, M.; Gomes, J. A.; Zerbetto, F. A Computational Analysis of the Insertion of Carbon Nanotubes into Cellular Membranes. *Biomaterials* **2011**, *32*, 7079−7085.
(16) Calvaresi, M.; Zerbetto, F. Baiting Proteins with $C_{60}$. *ACS Nano* **2010**, *4*, 2283−2299.
(17) Ehli, C.; Rahman, G. M. A.; Jux, N.; Balbinot, D.; Guldi, D. M.; Paolucci, F.; Marcaccio, M.; Paolucci, D.; Melle-Franco, M.; Zerbetto, F.; et al. Interactions in Single Wall Carbon Nanotubes/Pyrene/Porphyrin Nanohybrids. *J. Am. Chem. Soc.* **2006**, *128*, 11222−11231.
(18) Proença, M. F. J. R. P.; Araújo, R. F.; Silva, C. J.; Paiva, M. C.; Melle-Franco, M. Efficient Dispersion of Multi-Walled Carbon Nanotubes in Aqueous Solution by Non-Covalent Interaction with Perylene Bisimides. *RSC Adv.* **2013**, *3*, 24535−24542.
(19) Čížek, J. On the Correlation Problem in Atomic and Molecular Systems. Calculation of Wavefunction Components in Ursell-Type Expansion Using Quantum-Field Theoretical Methods. *J. Chem. Phys.* **1966**, *45*, 4256−4266.
(20) Paldus, J.; Čížek, J.; Shavitt, I. Correlation Problems in Atomic and Molecular Systems. IV. Extended Coupled-Pair Many-Electron Theory and its Application to the $BH_3$ Molecule. *Phys. Rev. A* **1972**, *5*, 50−67.
(21) Purvis, G. D.; Bartlett, R. J. A Full Coupled-Cluster Singles and Doubles Model: The Inclusion of Disconnected Triples. *J. Chem. Phys.* **1982**, *76*, 1910−1918.
(22) Strutyński, K.; Melle-Franco, M.; Gomes, J. A. N. F. New Parameterization Scheme of DFT-D for Graphitic Materials. *J. Phys. Chem. A* **2013**, *117*, 2844−2853.
(23) Grover, J. R.; Walters, E. A.; Hui, E. T. Dissociation Energies of the Benzene Dimer and Dimer Cation. *J. Phys. Chem.* **1987**, *91*, 3233−3237.
(24) Arunan, E.; Gutowsky, H. S. The Rotational Spectrum, Structure and Dynamics of a Benzene Dimer. *J. Chem. Phys.* **1993**, *98*, 4294−4296.
(25) Sinnokrot, M. O.; Sherrill, C. D. Highly Accurate Coupled Cluster Potential Energy Curves for the Benzene Dimer: Sandwich, T-Shaped, and Parallel-Displaced Configurations. *J. Phys. Chem. A* **2004**, *108*, 10200−10207.
(26) Pitoňák, M.; Neogrády, P.; Řezáč, J.; Jurečka, P.; Urban, M.; Hobza, P. Benzene Dimer: High-Level Wave Function and Density Functional Theory Calculations. *J. Chem. Theory Comput.* **2008**, *4*, 1829−1834.
(27) Bludský, O.; Rubeš, M.; Soldán, P.; Nachtigall, P. Investigation of the Benzene-Dimer Potential Energy Surface: DFT/CCSD(T) Correction Scheme. *J. Chem. Phys.* **2008**, *128*, 114102.
(28) Janowski, T.; Pulay, P. High Accuracy Benchmark Calculations on the Benzene Dimer Potential Energy Surface. *Chem. Phys. Lett.* **2007**, *447*, 27−32.
(29) Podeszwa, R.; Bukowski, R.; Szalewicz, K. Potential Energy Surface for the Benzene Dimer and Perturbational Analysis of $\pi\pi$ Interactions. *J. Phys. Chem. A* **2006**, *110*, 10345−10354.
(30) Valiev, M.; Bylaska, E.; Govind, N.; Kowalski, K.; Straatsma, T.; Van Dam, H.; Wang, D.; Nieplocha, J.; Apra, E.; Windus, T.; et al. NWChem: a Comprehensive and Scalable Open-Source Solution for Large Scale Molecular Simulations. *Comput. Phys. Commun.* **2010**, *181*, 1477−1489.
(31) Stewart, J. J. P. Optimization of Parameters for Semiempirical Methods V: Modification of NDDO Approximations and Application to 70 Elements. *J. Mol. Model.* **2007**, *13*, 1173−1213.
(32) Dewar, M. J. S.; Rzepa, H. S. Ground States of Molecules. 45. MNDO Results for Molecules Containing Beryllium. *J. Am. Chem. Soc.* **1978**, *100*, 777−784.
(33) Ponder, J. W.; Richards, F. M. An Efficient Newton-Like Method for Molecular Mechanics Energy Minimization of Large Molecules. *J. Comput. Chem.* **1987**, *8*, 1016−1024.
(34) Kundrot, C. E.; Ponder, J. W.; Richards, F. M. Algorithms for Calculating Excluded Volume and its Derivatives As a Function of Molecular Conformation and Their Use in Energy Minimization. *J. Comput. Chem.* **1991**, *12*, 402−409.
(35) Dudek, M. J.; Ponder, J. W. Accurate Modeling of the Intramolecular Electrostatic Energy of Proteins. *J. Comput. Chem.* **1995**, *16*, 791−816.
(36) Elstner, M.; Hobza, P.; Frauenheim, T.; Suhai, S.; Kaxiras, E. Hydrogen Bonding and Stacking Interactions of Nucleic Acid Base Pairs: A Density-Functional-Theory Based Treatment. *J. Chem. Phys.* **2001**, *114*, 5149−5155.
(37) Grimme, S. Density Functional Theory with London Dispersion Corrections. *Wiley Interdiscip. Rev.: Comput. Mol. Sci.* **2011**, *1*, 211−228.
(38) Pavone, M.; Rega, N.; Barone, V. Implementation and Validation of DFT-D for Molecular Vibrations and Dynamics: The Benzene Dimer As a Case Study. *Chem. Phys. Lett.* **2008**, *452*, 333−339.
(39) Korth, M.; Pitoňák, M.; Řezáč, J.; Hobza, P. A Transferable H-Bonding Correction for Semiempirical Quantum-Chemical Methods. *J. Chem. Theory Comput.* **2010**, *6*, 344−352.
(40) Korth, M. Third-Generation Hydrogen-Bonding Corrections for Semiempirical QM Methods and Force Fields. *J. Chem. Theory Comput.* **2010**, *6*, 3808−3816.
(41) Stewart, J. J. P. Optimization of Parameters for Semiempirical Methods VI: More Modifications to the NDDO Approximations and Re-Optimization of Parameters. *J. Mol. Model.* **2013**, *19*, 1−32.
(42) Dewar, M. J. S.; Zoebisch, E. G.; Healy, E. F.; Stewart, J. J. P. Development and Use of Quantum Mechanical Molecular Models. 76. AM1: A New General Purpose Quantum Mechanical Molecular Model. *J. Am. Chem. Soc.* **1985**, *107*, 3902−3909.
(43) Rocha, G. B.; Freire, R. O.; Simas, A. M.; Stewart, J. J. P. RM1: A Reparameterization of AM1 for H, C, N, O, P, S, F, Cl, Br, and I. *J. Comput. Chem.* **2006**, *27*, 1101−1111.
(44) Dewar, M. J. S.; Thiel, W. Ground States of Molecules. 38. the MNDO Method. Approximations and Parameters. *J. Am. Chem. Soc.* **1977**, *99*, 4899−4907.
(45) Allinger, N. L. Conformational Analysis. 130. MM2. a Hydrocarbon Force Field Utilizing V1 and V2 Torsional Terms. *J. Am. Chem. Soc.* **1977**, *99*, 8127−8134.
(46) Lii, J. H.; Allinger, N. L. Molecular Mechanics. The MM3 Force Field for Hydrocarbons. 2. Vibrational Frequencies and Thermodynamics. *J. Am. Chem. Soc.* **1989**, *111*, 8566−8575.
(47) MacKerell, A. D.; Bashford, D.; Bellott, M.; Dunbrack, R. L.; Evanseck, J. D.; Field, M. J.; Fischer, S.; Gao, J.; Guo, H.; Ha, S.; et al. All-Atom Empirical Potential for Molecular Modeling and Dynamics Studies of Proteins. *J. Phys. Chem. B* **1998**, *102*, 3586−3616.
(48) Foloppe, N.; MacKerell, A. D., Jr. All-Atom Empirical Force Field for Nucleic Acids: I. Parameter Optimization Based on Small Molecule and Condensed Phase Macromolecular Target Data. *J. Comput. Chem.* **2000**, *21*, 86−104.
(49) Vanommeslaeghe, K.; Hatcher, E.; Acharya, C.; Kundu, S.; Zhong, S.; Shim, J.; Darian, E.; Guvench, O.; Lopes, P.; Vorobyov, I.; et al. CHARMM General Force Field: A Force Field for Drug-Like Molecules Compatible with the CHARMM All-Atom Additive Biological Force Fields. *J. Comput. Chem.* **2010**, *31*, 671−690.
(50) Jorgensen, W. L.; Maxwell, D. S.; Tirado-Rives, J. Development and Testing of the OPLS All-Atom Force Field on Conformational Energetics and Properties of Organic Liquids. *J. Am. Chem. Soc.* **1996**, *118*, 11225−11236.
(51) Halgren, T. A. Merck Molecular Force Field. I. Basis, Form, Scope, Parameterization, and Performance of MMFF94. *J. Comput. Chem.* **1996**, *17*, 490−519.
(52) Dang, L. X.; Feller, D. Molecular Dynamics Study of Water-Benzene Interactions at the Liquid/Vapor Interface of Water. *J. Phys. Chem. B* **2000**, *104*, 4403−4407.

(53) Dang, L. X. Molecular Dynamics Study of Benzene−Benzene and Benzene−Potassium Ion Interactions Using Polarizable Potential Models. *J. Chem. Phys.* **2000**, *113*, 266.
(54) Ren, P.; Ponder, J. W. Consistent Treatment of Inter- and Intramolecular Polarization in Molecular Mechanics Calculations. *J. Comput. Chem.* **2002**, *23*, 1497−1506.
(55) Ren, P.; Ponder, J. W. Polarizable Atomic Multipole Water Model for Molecular Mechanics Simulation. *J. Phys. Chem. B* **2003**, *107*, 5933−5947.
(56) Ponder, J. W.; Case, D. A. Force Fields for Protein Simulations. *Adv. Protein Chem.* **2003**, *66*, 27−85.
(57) Allinger, N. L.; Yuh, Y. H.; Lii, J. H. Molecular Mechanics. The MM3 Force Field for Hydrocarbons. 1. *J. Am. Chem. Soc.* **1989**, *111*, 8551−8566.
(58) Kolmogorov, A. N.; Crespi, V. H. Registry-Dependent Interlayer Potential for Graphitic Systems. *Phys. Rev. B: Condens. Matter Mater. Phys.* **2005**, *71*, 235415.